Journal of Ceramic Processing Research. Vol. 16, No. 3, pp. 361~365 (2015)

J O U R N A L O F
Ceramic Processing Research

Characterization of anorthite-based porcelain prepared by using wollastonite as a calcium source

Shumei Wang[a,*], Xiaoling Qi[b], Jilin Hu[a] and Xiuying Tian[a]

[a]*Hunan Institute of Humanities, Science and Technology, Loudi 417001, China*

[b]*Energy Strategy Research Center, Guangzhou Institute of Energy Conversion, Chinese Academy of Sciences, Guangzhou 510540, China*

The porcelain based on anorthite ($CaO \cdot Al_2O_3 \cdot 2SiO_2$) has been developed using wollastonite ($CaO \cdot SiO_2$) as a calcium source. The slip casting was applied to obtain green body with high-strength. The sintering behaviors of the green specimens were evaluated by determining linear shrinkage, water absorption, bulk density and flexural strength. It was found that the anorthite porcelain fired at 1215 °C had excellent technical properties such as water absorption: 0.00% and flexural strength: 109.5 MPa. X-ray diffraction (XRD) and scanning electron microscopy (SEM) analysis results showed the high flexural strength was due to the densification of microstructures and the formation of high crystalline content in the porcelain body. In addition, thermal expansion performance and appearance quality of the final product were discussed.

Key words: Anorthite, Porcelain, Wollastonite, Calcium source.

Introduction

Whiteware ceramics are defined as highly dense products with white, translucent and fine texture, which is suitable for high-quality hotel and restaurant use (i.e., decorations and tablewares) [1]. Currently, hard porcelain and bone china are the two main types of commercial whitewares which dominate the upper end of the tableware market. Hard porcelain is a highly glassy whiteware (about 70% glass and 30% crystalline) with a low strength (~ 50 MPa) [2-4], so it is easily chipped. Bone china is highly crystalline material (about 70% crystalline and 30% glass) which is resistant to chipping (~ 100 MPa) [5]. However, bone china is only suitable for matching the low-temperature glaze (i.e., ≤ 1100 °C) due to its high thermal expansion coefficient (~ 8.4×10^{-6}/°C) [6] and is easily scratched, which limits service lifetime. Neither of these is really fit for severe service use, although both are extremely attractive whitewares.

Fortunately, a translucent whiteware, which combines the best features of bone china and hard porcelain was designed and developed by Capoglu and his cooperators [7-11]. The translucent whiteware consisted of anorthite ($CaO \cdot Al_2O_3 \cdot 2SiO_2$) and mullite ($3Al_2O_3 \cdot 2SiO_2$) crystalline phases with a glassy phase with high crystalline to glassy phase ratio, whose maximum flexural strength can reach about 135 MPa. However, the cost of preparation was higher than the presently used bone china due to the need for the prefired materials, which were fabricated by highly pure chemical materials at 1370 °C. Cheng *et al.* [12] reported a ceramic material based on anorthite as a porcelain tableware, which was obtained from a mixture of ball clay, quartz, calcite, feldspar and alumina by slip casting and sintering at 1230 °C. This material was composed of single anorthite phase, possessing high crystalline to glassy phase ratio, which had high whiteness and high strength (~ 103 MPa). Nonetheless, calcite ($CaCO_3$) as a raw material could cause a negative effect on the sintering character of the anorthite ceramic (i.e., high linear shrinkage and porous microstructures) due to the decomposition reaction of calcite at high temperatures. Wollastonite ($CaO \cdot SiO_2$) is one of the mineral materials which has widely use in the production of ceramics [13-15]. In the present work, the anorthite porcelain was fabricated by adding wollastonite as a calcium source, whose technical properties and microstructures were investigated by sintering study, flexural strength measurement, X-ray diffraction (XRD) and scanning electron microscopy (SEM) techniques. In addition, thermal expansion performance and appearance quality of the final product were discussed.

Experimental Procedure

Ball clay, quartz, feldspar and wollastonite are used as the starting raw materials, which is from Sitong Group Co. LTD., Guangdong, China. In addition, earlier study [11, 16] demonstrated that the anorthite crystals were only a few microns in length and were not capable

*Corresponding author:
Tel : +86-18573838559
Fax: +86-18573838559
E-mail: wwzscut@gmail.com

Table 1. Chemical composition of the used raw materials.

Constituents (wt.%)	Ball clay	Quartz	Wollastonite	Alumina	Feldspar
SiO_2	48.61	98.38	50.13	–	65.56
Al_2O_3	36.14	1.02	0.92	99.0	18.85
Fe_2O_3	0.21	0.03	0.20	–	0.08
TiO_2	0.14	0.01	0.02	–	0.02
CaO	0.16	0.08	44.80	–	0.23
MgO	0.21	0.02	0.82	–	0.03
K_2O	0.98	0.07	–	–	12.39
Na_2O	0.24	0.04	–	–	2.28
Ignition loss	12.7	0.23	3.21	–	0.56

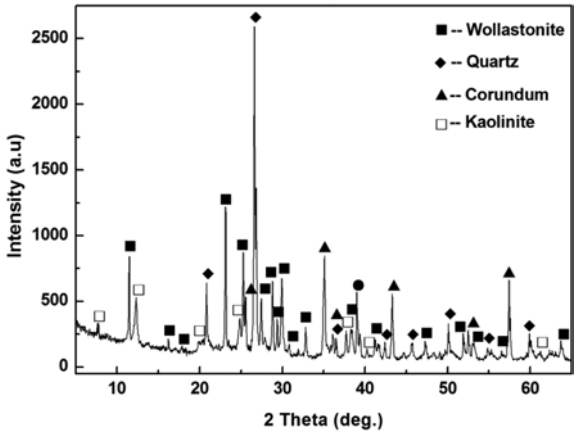

Fig. 1. XRD pattern of the green body.

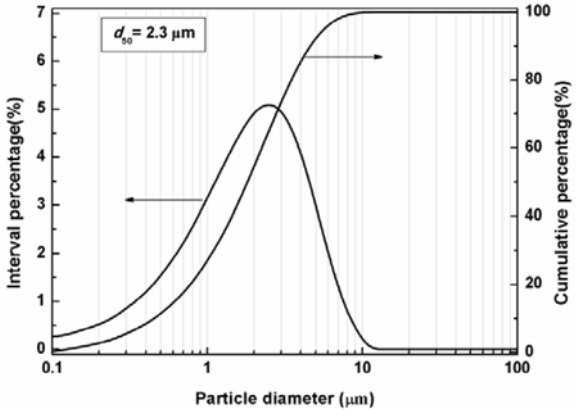

Fig. 2. The particle size distribution of the milled slurry.

enough to resist the pyroplastic deformation during firings. To resist high-temperature deformation, small amount of industrial alumina (Veking materials Co. LTD., Hangzhou, China) is added as a source of aluminium to increase the viscosity of melted liquid. The chemical composition of the used raw materials is shown in Table 1. The green body used in this study consisted of 20 wt.% ball clay, 7 wt.% quartz sand, 18 wt.% feldspar, 40 wt.% wollastonite and 15 wt.% industrial alumina. Fig. 1 shows X-ray diffraction (XRD) pattern of the green body. The analysis result indicates that quartz (SiO_2) was the major phase with a small amount of wollastonite ($CaSiO_3$), corundum (Al_2O_3) and kaolinite ($Al_2Si_2O_5(OH)_4$).

The raw materials were wet mixed and milled in a planetary mixer with zirconia ball millstone for 6 h. The particle size distributions of the milled slurry were analysed by a BT-9300S model laser diffraction particle size analyzer (Dangdong Bettersize Instruments Ltd., China), and the result is given in Fig. 2. A log-normal distribution presenting one maximum point, and the curve of cumulative distribution is also presented. The particle sizes are less than 10 μm, which are centred at around 1-5 μm.

The slip casting was used for forming, which could obtain green body with high-strength [17, 18]. The green specimens were casted in a plaster mold into rectangular blocks of 60 mm × 60 mm × 10 mm dimensions. After withdrawal of the mold, specimens were dried at 90 ºC for 12 h. Subsequently, the firing process was performed in an electric furnace at temperatures from 1170 to 1245 ºC with 15 ºC intervals for 1 h.

The crystalline phases of the samples were determined by an X-ray diffractometer (XRD, Philips PW-1710, the Netherlands) using Cu *K*a radiation. The thermal analysis was investigated by a simultaneous thermogravimetry and differential scanning calorimetry (DT-DSC, STA449C, Netzsch Instruments Ltd., Germany), at a heating rate of 10 ºC/min, in air atmosphere. The microstructure morphology of the sintered simples was observed by scanning electron microscopy (SEM, Philips L30FEG, the Netherlands). The sintering behaviors of the specimens such as linear shrinkage, water absorption and bulk density were determined according to the Archimedes method [19]. The flexural strength of the fired specimens was measured by with the three-point bending test (Model5569, Instron Ltd., USA) at a loading rate of 0.5 mm/min. The thermal expansion coefficient of sintered specimens was measured between room temperature and 500 ºC using a mode DIL402EP thermal dilatometer (Netzsch Instruments Ltd., Germany). The color of the fired samples was determined according to the CIELAB color scale on a mode X-Rite Color Premier 8200 reflection differential colorimeter (X-Rite Co., USA).

Results and Discussion

Fig. 3 shows the TG-DSC curves of the green body. The TG curve displays a relatively continuous weight loss. The overall weight loss is about 4%. The DSC curve shows an endothermal peak at 90.4 ºC, corresponding to the removal of residual water, and an exothermic peak at 344.6 ºC due to the burning out of organic compounds. The endothermal peak at 497.3 ºC results from the dehydroxylation process of kaolinite. At 575.3 ºC, the small endothermic peak is attributed to

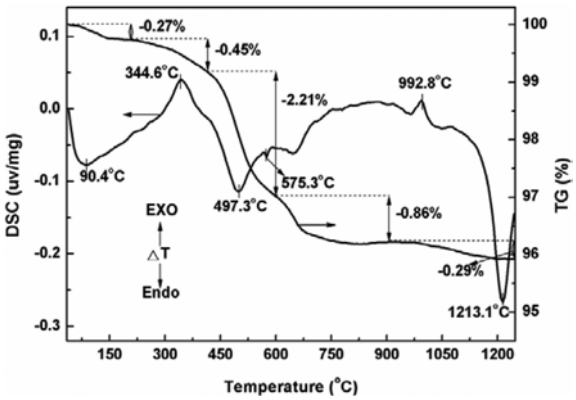

Fig. 3. TG-DSC curves of the green body.

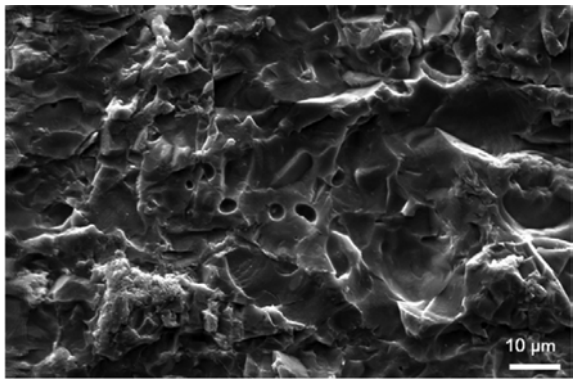

Fig. 4. SEM image of the fracture surface for the sample fired at 1215 °C.

Table 2. Sintering characters and flexural strength of the samples fired at different temperatures.

Property	Temperature (°C)					
	1170	1185	1200	1215	1230	1245
Linear shrinkage (%)	8.51	8.60	8.76	8.85	8.82	8.80
Water absorption (%)	0.83	0.28	0.14	0.00	0.00	0.08
Bulk density (g/cm^3)	2.20	2.30	2.37	2.45	2.39	2.36
Flexural strength (MPa)	91.4	94.4	96.9	109.5	106.0	102.9

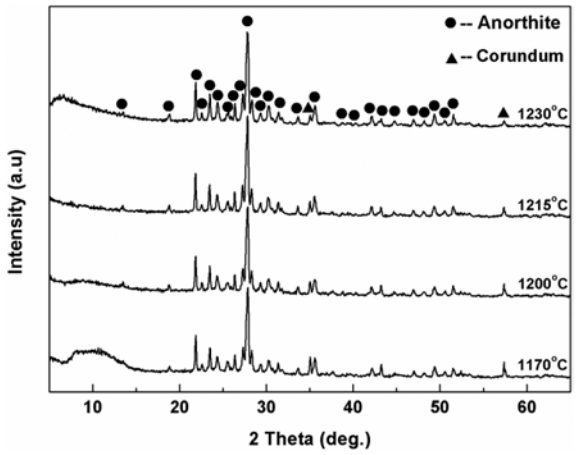

Fig. 5. XRD patterns of the samples fired at different temperatures.

the polymorphic transformation of α-β quartz. The exothermal peak observed at 992.8 °C is due to the formation of anorthite ($CaO{\cdot}Al_2O_3 \cdot 2SiO_2$). Kobayashi *et al.* [20] reported the production of dense anorthite ceramics by sintering at 1000 °C, using kaolin and finely milled calcite. According to the Al_2O_3-SiO_2-CaO phase diagram, pure anorthite melts congruently at 1553 °C [21], which makes it interesting for producing wall tiles, floor tiles and porcelain. And then, a steep descent at higher temperatures indicates the formation of a liquid phase mainly derived from the feldspar component [22]. In general, the melted glassy phase plays a flux role and makes the material densification easily.

Table 2 shows the sintering characters (i.e., linear shrinkage, water absorption and bulk density) of the samples fired at 1170, 1185, 1200, 1215, 1230 and 1245 °C, respectively. The linear shrinkage slightly increases and reaches the maximum value (8.85%) at 1125 °C, and then decreases with the increasing firing temperature. For the water absorption, the result indicates that increasing temperature has a good effect on the sintering behavior. The ISO 10545 standard prescribes a maximum water absorption value of 0.5% for porcelain. In this work, the water absorption of the fired bodies achieves the standard's requirement, when the firing temperature reaches 1185 °C. In addition, the variation trend of bulk density is similar to that of linear shrinkage. There presents a continuous increase in bulk density up to 1215 °C and a volume expansion takes place for sintering after this temperature point, reducing the bulk density from 2.45 to 2.36 g/cm^3. Fig. 4 shows SEM image of the fracture surface for the sample fired at 1215 °C. The microstructure with a rather smooth fracture surface is very homogeneous, attesting to the formation of abundent liquid phase during firing. In addition, the pores are round and isolated, which also implies the sample fired at 1215 °C has an excellent sintering performance.

In addition, Table 2 also shows the flexural strength of the samples fired at the temperature range of 1170-1245 °C. The flexural strength initially increases and reaches the maximum value (109.5 MPa) at 1215 °C, which is close to that of bone china and much higher than that of hard porcelain (~ 50 MPa) [4], and then slowly decreases with the increasing firing temperature. Flexural strength showed a consistent relation with bulk density, as expected. In fact, the high strength value of bone china compared to hard porcelain is attributed to its high crystalline content [5]. Fig. 5 shows XRD patterns of the samples fired at different temperatures. For all samples, anorthite is always the

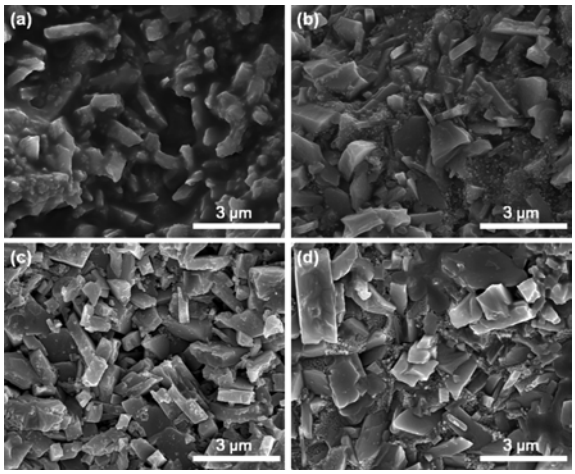

Fig. 6. SEM images of the sample fired at (a) 1170, (b) 1200, (c) and (d) 1230 °C, respectively.

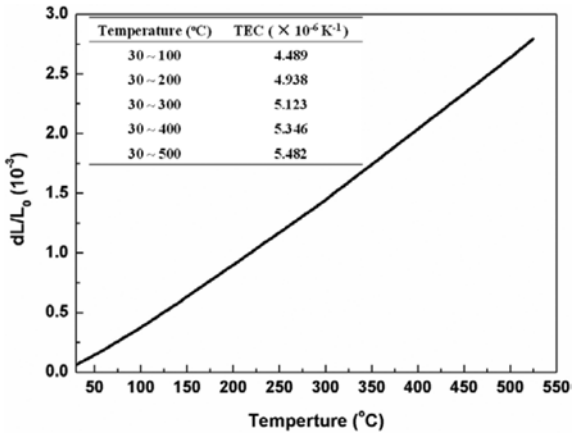

Fig. 7. Thermal expansion ratio curve of the sample fired at 1215 °C.

major phase with a small amount of corundum. However, the XRD pattern of the sample fired at 1170 °C presents a broad peak about $2\theta \approx 10^{o}$, which means that there exists quite an amount of glassy phase. And then, the broad peak vanishes above 1200 °C. The diffraction intensity of corundum decreases and that of anorthite increases, which means the content of anorthite increases with the increasing temperature. The previous literatures [23, 24] implied that anorthite also could be formed by the crystallization from the glassy phase during the firing process. However, the viscosity of glassy phase is quite rapidly decreased above 1230 °C, which makes anorthite particles melt easily leading to the increase of glassy phase.

Fig. 6 shows SEM images of the fracture surface for the samples fired at different temperatures. All samples were chemically etched by 5% hydrofluoric acid solution for 30 seconds. There are a large amount of the crystal particles wrapped in the glassy melt in Figs. 6a, b and d. The sample fired at 1215 °C clearly presents cuboid or lamellar anorthite crystals in Fig. 6c, which possesses a high crystalline to glass ratio. The high flexural strength of the sample fired at 1215 °C might be due to the formation of high crystalline content in the porcelain body, which is consistent with the previous research results [25, 26].

Table 3. Whiteness of the sample fired at 1215 °C.

Type of porcelain	*L**	*a**	*b**	Source
Bone china	93.15	–0.43	3.17	[9]
Hard porcelain	86.71	–1.12	2.40	[9]
Anorthite porcelain	91.01	–0.89	4.86	This work

Fig. 7 shows the thermal expansion coefficient (TEC) curve of the sample fired at 1215 °C. The expansion ratios are almost linear increase over the entire measured temperature range (30-500 °C). For practical application of high-strength porcelain for tableware, thermal expansion below 150 °C is important in order to withstand the thermal shock of heat disinfection or washing [27]. The average TEC values of the simple below 300 °C are calculated as 5.123×10^{-6} K^{-1}. While the TEC for glasses of the compositions detected in common glaze from 20 to 350 °C were calculated to be $\sim 4.5 \times 10^{-6}$ K^{-1} [28]. So, the anorthite porcelain can be matched with applicable glaze easily. Moreover, this relatively low TEC also indicates that the materials would be very resistant to being thermally shocked.

The whiteness of porcelain whiteware is crucial for its marketing [29]. To explain quantitatively the whiteness of the prepared anorthite porcelain, the difference in whiteness was compared with commercial bone china and hard porcelain, whose data were from reference 9. The color difference values (*a**, *b**) and the *L** parameter (whiteness) are summarized in Table 3. The result shows that negative value of *a** and positive value of *b** were measured for the prepared anorthite porcelain, indicating that the value position lies in the upper left quadrant (green and yellow region) with coordinates. Low values of *a** and *b** for the prepared anorthite porcelain also indicates a very low coloring grade. Meanwhile, its whiteness value reaches ~ 91, which is between hard porcelain (~ 86) and bone china (~ 93). Thus, the prepared anorthite porcelain has a high appearance quality.

Conclusions

In the present study, anorthite porcelain was prepared by slip casting and sintering from a mixture of ball clay, quartz, feldspar, industrial alumina and wollastonite. When the firing temperature reached 1215 °C, the sample had optimal technical properties such as water absorption: 0.00%, bulk density: 2.45 g/cm^3 and flexural strength: 109.5 MPa. The XRD result showed that anorthite is the major phase with a small amount of corundum in the anorthite porcelain. The high flexural strength was due to the densification of microstructures and the formation of high crystalline content in the

porcelain body. In addition, the anorthite porcelain had a relatively low thermal expansion coefficient (5.123×10^{-6} K^{-1}) in the temperature range from 30 to 300 °C, which can be matched with applicable glaze easily. Meanwhile, the whiteness value of the anorthite porcelain reached ~ 91, which is between hard porcelain (~ 86) and bone china (~ 93). Thus, the prepared anorthite porcelain has a high appearance quality.

Acknowledgments

This work was supported by the ChanXueYan Special Funds of Guangdong (No. 2012B091100306).

References

1. W.M. Carty, and U. Senapati, J. Am. Ceram. Soc. 81 (1998) 3-20.
2. S.R. Braganca, and C.P. Bergmann, Ceram. Int. 29 (2003) 801-806.
3. O.I. Ece, and Z. Nakagawa, Ceram. Int. 28 (2002) 131-140.
4. Y. Kobayashi, O. Ohira, Y. Ohashi, and E. Kato, J. Am. Ceram. Soc. 75 (1992) 1801-1806.
5. A.C.B. Ustundag, Y.K. Tur, and A. Capoglu, J. Am. Ceram. Soc. 26 (2006) 167-177.
6. Y. Iqbal, P.F. Messer, and W.E. Lee, Br. Ceram. Trans. 99 (2000) 110-116.
7. A. Capoglu, and P.F. Messer, J. Eur. Ceram. Soc. 24 (2004) 2067-2072.
8. A. Capoglu, Key. Eng. Mater. 264-268 (2004) 1585-1588.
9. A. Capoglu, J. Eur. Ceram. Soc. 31 (2010) 321-329.
10. A. Capoglu, and M.U. Taskiran, Key. Eng. Mater. 264-268 (2004) 1621-1624.
11. C.B. Ustundag, Y.K. Tur, and A. Capoglu, J. Eur. Ceram. Soc. 26 (2006) 167-177.
12. X.S. Cheng, S.J. Ke, Q.H. Wang, H. Wang, A.Z. Shui, and P.A. Liu, Ceram. Inter. 38 (2012) 3227-3235.
13. M. Sathiyakumar, and F.D. Gnanam, Ceram. Inter. 29 (2003) 869-873.
14. B. Baran, Y. Sarýkaya, T. Alemdaroglu, and M. Onal, J. Eur. Ceram. Soc. 23 (2003) 2061-2066.
15. M. Magallanes-Perdomo, Z.B. Luklinska, A.H.De. Aza, R.G. Carrodeguas, S.De. Aza, and P. Pena, J. Eur. Ceram. Soc. 31 (2011) 1549-1561.
16. R. Ponraj, S.R. Iyer, and V.M. Radhakrishnan, J. Mater. Sci. 29 (1994) 4385-4392.
17. P.T. Weon, K. Kimura, and K. Jinnal, J. Mater. Sci. 37 (2002) 1273-1279.
18. R.D. Rawlings, J.P. Wu, and A.R. Boccaccini, J. Mater. Sci. 41 (2006) 733-761.
19. A. Christogerou, T. Kavas, Y. Pontikes, S. Koyas, Y. Tabak, and G.N. Angelopoulos, Ceram. Inter. 35 (2009) 447-452.
20. Y. Kobayashi, and E. Kato, J. Am. Ceram. Soc. 77 (1994) 833-834.
21. S. Kurama, and E. Ozel, Ceram. Int. 35 (2009) 827-830.
22. J. Martín-Márquez, J.Ma. Rincón, and M. Romero, Ceram. Inter. 34 (2008) 1867-1873.
23. K. Andreas, H. Thomas, and K. Jens, J. Eur. Ceram. Soc. 29 (2009) 207-221.
24. S.A.F. Batista, P.F. Messer, and R.J. Hand, Bri. Ceram. Trans. 100 (2001) 256-259.
25. M.U. Taskiran, N. Demirkol, and A. Capoglu, J. Eur. Ceram. Soc. 25 (2005) 293-300.
26. A. Capoglu, and M.U. Taskiran, Key. Eng. Mater. 264-268 (2004) 1495-1498.
27. K. Yuichi, Y. Mitsunori, N. Mikio, O. Osamu, and I. Hirofumi, J. Ceram. Soc. Jap. 111 (2003) 872-877.
28. A. Capoglu, J. Eur. Ceram. Soc. 25 (2005) 3157-3162.
29. Kr.D. Swapan, and D. Kausik, Thermochim. Acta. 406 (2003) 199-206.